# OPTICAL OBSERVABLES IN STARS WITH NON-STATIONARY ATMOSPHERES

R. W. Hillendahl
Science Applications, Inc.
2680 Hanover Street
Palo Alto, California

## ABSTRACT

Experience gained by use of cepheid modeling codes to predict the dimensional and photometric behavior of nuclear fireballs is used as a means of validating various computational techniques used in the cepheid codes. Predicted results from cepheid models are compared with observations of the continuum and lines in an effort to demonstrate that the atmospheric phenomena in cepheids are quite complex but that they can be quantitatively modeled. It is hoped that the discussion may provide guidance for cepheid observers.

# INTRODUCTION

The application of the artificial viscosity technique (Von Neumann and Richtmyer, 1950) to the explicit hydrodynamic modeling of spherical systems (Brode, 1955) represents a fundamental milestone in computer modeling. Subsequently, Brode combined radiative diffusion with the hydrodynamic motion (Brode, 1956-1957), having incorporated the implicit Henyey method (Henyey, Le Levier, Levee, Böhm, and Wilets, 1959) with the assistance of Le Levier. He then produced the first radiation-hydrodynamic models of the fireball which results from a nuclear explosion in the atmosphere (Brode, 1958, 1959a, 1959b). Christy (Christy, 1964, 1967) later modified the Brode technique and applied it to his pulsation studies of stellar envelopes and thus laid the foundation for many subsequent investigations.

During the period where Brode was producing his models of fireballs, the present author was engaged in making astrophysical and photgraphic observations of fireballs (Hillendahl, 1959). This afforded an opportunity for the quantitative comparison of Brode's modeling techniques with observational data having a much higher degree of precision than is possible from stellar observations. The results of such comparisons validated the hydrodynamic and radiative diffusion techniques used by Brode, but identified the need for an improved treatment of the radiative transport in the observable atmospheric layers. As a student of Henyey, the author developed a radiation-hydrodynamics technique designed to treat all regions of the star (Hillendahl, 1962,

1964) which was used both for cepheid modeling and in a relaxation technique (Hillendahl, 1965a) for the study of stable Henyey models. This "SUPER NOVA" code was later adapted for use in an extensive study of fireballs (Hillendahl, 1965b, 1966).

This presentation provides a brief review of selected numerical and interpretational techniques which have a proven usefullness, and a description of some physical processes which the computer models predict to occur in stellar atmospheres.

It is well established that some features of stellar models are sensitive to particular details of the computational technique. For example, the behavior of a cepheid model employing the artificial viscosity technique may be dependent upon the formulation used. One approach to resolving such difficulties is a careful comparison against data. Another approach is for a number of modelers to use their codes to model a well defined test case so that differences due to computational techniques can be identified. Both techniques have been used extensively by the fireball modelers (Brode, 1965). Much of this material is no longer subject to government security restrictions. The brief exposition given here is intended to allow the stellar modeling community to benefit from these findings and to reduce the number of uncertainties in their models.

Brode (1965) compared "standard model" calculations performed by a number of investigators. He demonstrated conclusively the importance of an accurate equation of state which includes the relevant dissociation and ionization processes. He also demonstrated that equation of state must maintain the correct relationship between the pressure P and internal energy E if predicted hydrodynamic phenomena are to correspond to the experimental observations. Thus if curve fits or data tables are used in the computational model, care must be taken to see that the correct relationship between P and E is reproduced. False hydrodynamic signals may otherwise be produced.

The artificial viscosity technique is a useful device in the treatment of shock discontinuities. The literature abounds with various versions referred to as "linear", "quadratic", "quartic"; various versions formulated in terms of velocity gradients and/or compression ratios; and various recommended values for the damping constant. Many of these have proven to be applicable over limited ranges of the variables or only under limited circumstances. The formulation discussed by Richtmyer (Richtmyer and Morton, 1967, page 319) has been shown (Hillendahl, 1965b) to accurately (±2%) reproduce, without adjustment, the shock front properties in a nuclear fireball while the shock pressure changes some six orders of magnitude. Furthermore, the shock structure produced by the model satisfies the Rankine-Hugeniot conditions to a high degree of accuracy. One has no reason to expect that the Richtmyer formulation would not perform equally well in stellar calculations.

A useful technique for locating shock fronts and related phenomena at a given epoch is a listing of the quantity Q/P as a function of mass or radius, where Q is the artificial pressure and P is the gas pressure. Non-zero values, which indicate a compression of the gas, are then easily identified. The largest value of Q/P occurs as the shock front is in the process of transversing a given zone. This behavior has been employed as a shock locator (Simpson, 1973) and as a print control to cause the radial structure to be displayed at the instant the shock compression of a given zone is complete.

In a model using the artificial viscosity technique, the Rankine-Hugeniot conditions are satisfied on a time averaged basis, but not always on an instantaneous basis. Use of the Simpson technique automatically selects epochs when these conditions are satisfied and make the data analysis process simpler.

In the interest of conserving computer time, most modern codes employ continuously variable time steps chosen to satisfy various hydrodynamic, radiative, or energetic criteria. With this capability available, the last time step during compression of the zone can be chosen so as to cause a print-out precisely at the end of the compression of the zone in question. The effects of finite zoning upon the time history of the shock location and the shock properties are then minimized.

Use of the artificial viscosity technique results in a compression of the material ahead of the true shock front. This compression results also in a false temperature rise. At temperatures lower than about $15,000^{\circ}K$, the absorption coefficient of the gas is very temperature dependent ($\sim T^{9}$) and the artificial compression can thus result in the creation of false optical properties ahead of the shock. Under conditions where the pre-shock gas would be transparent, and the post-shock gas opaque, an artificial photosphere will will be created having a temperature lower than the post-shock temperature. The emergent flux is then depressed. Thus a sudden depression in the computed light output of a cepheid model may be associated with the emergence of a shock wave.

Two aspects of this distortion of the temperature profile by the artificial viscosity are of interest. Simpson (1973) conducted numerical experiments on fireball shock waves in which he artificially increased the opacity by a factor of $10^6$. When the post-shock temperature was below $10^{4\circ}$K, he found that this opacity increase had a negligible effect upon the temperature and density profiles because the radiative transfer could not compete with the hydrodynamics at lower temperatures. It is clear, however, that the false compression due to the artificial viscosity does affect the radial heat flow, but only in a transient manner. By separately printing out the hydrodynamic and radiative terms of the energy equation, one can assess their relative importance and also to determine whether a particular configuration exists long enough to result in a distortion of the temperature profile. This type of distortion has not proven to be important if the zone structure if fine enough to meet the other requirements of good modeling.

If one desires to obtain high quality optical output as a shock wave emerges through the photosphere, it may be necessary to correct the distorted regions of the temperature, density, and velocity profiles. The quantity Q/P described above is very useful in controlling this process. When the artificial pressure is small compared to the gas pressure, no correction is needed. When corrections are needed, the "distorted" values are temporarily stored so that they can be

recovered in order to proceed with the pulsation model. Substitute values are then used to compute the observable properties at the epoch in question. Some investigators, e.g., C. G. Davis (LASL), prefer not to interrupt the main calculation. They store the configuration at epochs of interst for later "snap-shot" light output calculations.

The estimation of these corrected values is relatively easy in fireball modeling as the profiles ahead of the shock are usually known. Two techniques have been used in cepheid modeling: space extrapolation and time extrapolation. In both techniques data prior to the artificial viscosity distortion are used to predict the needed substitute values. The choice between the two methods is made on the basis of the slowest rate of change of the zone properties in either time or space.

The appearance of a region where Q/P is greater than zero may not indicate the presence of a shock front. If the disturbance moves toward a region of lower pressure it is likely to be a shock wave. If the disturbance moves toward a region of higher pressure, it may be an unloading or rarefaction wave. The optical properties of various waves are discussed below.

Because of the demonstrated inability of radiative diffusion techniques to adequately reproduce the optical observables from nuclear fireballs, it is to be expected that such techniques would also have similar deficiencies when applied to the atmospheres pulsating stars. Here one is faced with the classical problem of radiative

transfer, i.e., the equation of transfer of radiation describes change in the intensity for a given radiation frequency and along a given direction in space. To obtain the radiative flux divergence it is necessary to integrate over both the frequency and over all directions in space. One approach is to use a large number of rays at various angles and a large number of radiation frequencies. One fireball code employing this approach used about 250 hours of machine time to model the equivalent of one period of a star. The SUPER NOVA technique (Hillendahl, 1964, 1965) produced virtually indistinguishable results and utilized only about 1 hour of machine time (about 5 minutes equivalent CDC 7600 time). In this technique, the source function is expanded in a Taylor series, in terms of optical distance, centered on each zone boundary. An integral formulation of the equation of transfer is applied to the finite zone configuration in an equivalent ray approximation. This results in direct and chord transmission terms, and in a series of emission terms. In the optically thin extreme, the zero order emission term reproduces the Planck approximation. In the optically thick extreme, the first order term reproduces the Rosseland approximation. Higher order terms are truncated. The formulation leads to a novel technique for spectral averaging that is a finite zone equivalent of the Chandrasekhar or flux weighted mean.

An important feature of this formulation is that it provides a reasonably high order solution to the well known problem in cepheid modeling in which the opacity increases very rapidly at the photosphere causing one zone to be very optically thick and the next exterior

zone to be nearly transparent. This difficulty arises when a Rosseland mean or equivalent opacity approximation is used in which the opacity of a zone depends only upon the local temperature. The zone exterior to the photosphere has a low temperature and thus a low opacity. It cannot absorb radiation and must depend upon hydrodynamic compression to heat it sufficiently to increase its opacity so that the absorption of outward flowing radiation can begin. The SUPER NOVA formulation employs transmission functions for the outwardly directed radiation which are of the form

$$T = \frac{\int_{\lambda} B_{\lambda}(T_s)\ \exp(-\mu_{\lambda}\ell)d\lambda}{\int_{\lambda} B_{\lambda}(T_s)\ d\lambda}$$

wehre T is the outward transmission

$\ell$ is the zone thickness along the characteristic ray

$T_s$ is the temperature of the next interior zone

$B_{\lambda}$ is the Planck function

$\lambda$ is the wavelength

$\mu_{\lambda}$ is the local spectral absorption coefficient and is a function of the local gas density and temperature.

In common with the Planck and Rosseland means, the transmission function depends upon the local temperature and density of the gas. But it also depends upon the zone thickness and temperature of the "source" zone. It is therefore a function of four variables instead of two.

In practice these functions are computed in great detail in a preliminary calculation from detailed spectral absorption coefficient codes. Because of the existence of absorption edges, and because the Planck distribution is a function of $\lambda T$, it is convenient to index these precomputed data in terms of $T_s$ and $\lambda_z$, where $T_s$ is a property of the source zone and $\lambda_z$ depends only on the properties of the zone whose transmission is desired. This affords a reduction in complexity which makes the method workable.

Other investigators have used the Rosseland approximation in the interior and a finite number of spectral bands in and exterior to the photosphere. Both of these methods provide for the non-gray radiative heating of the gas prior to shock compression which cannot be accounted for with an unmodified diffusion approximation. With the great increase in computer capabilities since the SUPER NOVA technique was developed, the later technique is probably to be preferred because less effort is involved when the chemical composition is changed.

# ATMOSPHERIC OBSERVABLES

The fireball from a nuclear explosion is a relatively simple object in the astrophysical sense. If one considers only relatively high energy explosions, then the nuclear device simply causes the formation of a hot isothermal sphere of air and exerts no significant influence on the subsequent hydrodynamic and radiative development which follows. Even so, this relatively simple object exhibits a great deal of structure involving periods of radiative growth, the formation of shocks, hydrodynamic growth, rarefaction waves, radiative cooling waves, dissociation fronts that mimic H II regions, absorption shells, and similar phenomena.

Pulsating stars are much more complex objects than fireballs because the gas ahead of the expanding shock front is not of uniform density. One would, therefore, expect that the atmospheric phenomena might be even more complex than in the fireball.

In the case of the fireball, the author (Hillendahl 1966) demonstrated the capability of the SUPER NOVA cepheid modeling code (as modified for air) to quantitatively model the atmospheric phenomena which occur in fireballs. Both the hydrodynamic and radiative phenomena predicted by the code are verified by photographic and photometric measurements. If the same modeling techniques are used on a cepheid, what type of atmospheric phenomena are predicted? Can any or all of these phenomena be confirmed by observation?

In an attempt to answer these questions, a number of models of a 7.6 day cepheid were computed and analyzed using analysis techniques developed from fireball experience. The model consisted of a periodic envelope model supplied by Christy (1968) to which an extended atmosphere was appended. The augmented models remain periodic in the denser envelope regions, but never reach a completely repetitive behavior in the extreme outer layers where mass loss is predicted to occur (Hillendahl 1970). The physical phenomena discussed below are not dependent upon the precise periodic behavior of the star.

Figure 1 shows the radius-time history of every fifth mass point in the computed model. Although several shock fronts (S1, S2, S3) have been labeled, it is clear that little, if any, detailed information can be obtained or illustrated on such a radius-time display. Figure 2 shows the same model displayed in a different fashion. Various shock fronts and rarefaction waves which have been identified are labeled S and R, respectively. The photosphere ($\tau$=1) has been indicated by the continuous line.

For a shock front to be observable in continuum light, it must occupy the photospheric region of the star. In the model shown, the thickness of the photosphere is from 1 to 2 mass zones throughout the cycle. Thus, the model predicts that shock waves, including the very strong shock S2 which "drives" the pulsation, will occupy the photosphere only for very brief intervals in time, i.e., of the order of 1-3 hours in a 7-day cepheid.

Since the cepheid light curve rises over a time interval of several days, it is clear that the light being observed is not being emitted by the shock front itself.

In the nuclear fireball, the rapid rise in the light curve, which follows after the expanding shock becomes transparent, results from the rapid density decrease on the back side of the shock front. Interior to the shock front, the density decreases rapidly in the inward direction, while the temperature rises rapidly so as to maintain a nearly constant pressure behind the shock. Just after shock transparency, the photosphere resides in a layer of gas just behind the shock front. As the whole system expands radially, the density at every point on the back of the shock decreases with time in order to conserve mass. This decrease in density lowers the opacity of the photospheric layer and causes the photosphere to progress inward in terms of mass and toward regions of higher temperature. Since the opacity depends strongly on the temperature and weakly on the density, only a slight increase in temperature is needed to compensate for the density decrease. Thus, the photosphere moves inward relatively slowly in terms of the mass coordinate, and actually moves outward in terms of radius.

During rising light in the fireball, the radius of the photosphere increases by about a factor of two, while the light output may increase a factor of 50 or more. It is clearly the increase in temperature which is responsible for most of the light increase. This being the case, one expects, and observes, a larger

amplitude for wavelengths to the short wavelength side of the maximum of the Planck function, i.e., the amplitude is larger in blue light just as in the cepheid.

The model calculations predict that the same mechanism operates during the rising light phases in a cepheid. During these phases, the models predict an abrupt spatial density decrease on the back side of the shock front. If one follows a given shock as it emerges from deep in the star, it is found that the density profile behind the shock changes rapidly with radius. In most regions of the star, the density minimum behind the shock is only about 30% below the shock front density. However, when the gas undergoes thermal ionization as it crosses the shock, the density minimum is as much as a factor of 10 lower than the shock front density. This phenomenon is easily explained. The ionization increases the number of particles and hence the gas pressure. The increased pressure forces the gas to expand thus lowering its density.

Clearly then, the amplitude of the light curve depends upon the magnitude of the density decrease behind the shock, which in turn depends upon the shock compression to dissociate or ionize the gas. One would, therefore, expect pulsating stars to be highly visible if an ionization or dissociation zone happens to occur near the photospheric layers. Estimates of the light amplitude caused by shock emergence when ionization is not present are of the order of 0.1 mag. (Hillendahl 1969).

Because of the real possibility that considerations such as these might contribute to an observational selection bias, further investigation seems to be indicated.

Maximum light (phase 0.0) in the cepheid apparently occurs when the photosphere has progressed down the back side of the shock density profile and arrives at the density minimum. The previously discussed process responsible for rising light is then interrupted. The model calculations then indicate an unloading or rarefaction wave then dominates the atmospheric phenomena (Hillendahl 1969, 1970). Figure 3 shows the density and temperature profiles at phase 0.103 during the rarefaction wave R2 (see Fig. 2). The density spike shown is not the shock wave, which has traversed the atmosphere, but is a residual structure resulting from the previously described series of events. The density minimum has a value of $5 \times 10^{-10}$ gm $cm^{-3}$. The dashed box labeled "54" is a graphical device for denoting the mass zone in which the photosphere occurs. Its width is that of the mass zone and its height is a factor of 6. Graphs similar to Figure 3 have been used to construct a 16 mm movie which shows the atmospheric structure throughout the entire period.

The strange atmospheric profiles shown in Figure 3 provided the nucleus for an idea for the construction of "dynamic" model atmospheres (Hillendahl 1968) for cepheids. The temperature external to the photosphere is practically uniform, while the density profile is slab-like in appearance. Since the absorption

coefficient depends strongly on the temperature and weakly on the density, the profile was approximated by a slab of uniform temperature and density overlying a blackbody photosphere.

Using a very detailed code for computing the spectral absorption coefficients, simple models were constructed using the photospheric temperature $T_b$ and the slab temperature $T_a$, density $\rho_a$, and thickness $\Delta_x$ as variable parameters (Hillendahl 1968). Table 1 shows the results obtained using the "dynamic" model technique to match the spectral scanner data (Oke 1961) for Eta Aquilae. Outside the Balmer line blanketed region, the agreement is relatively good at all but a few wavelengths. The same technique was applied indiscriminately at all phases with the results shown in Table 2. At 14 of the 20 phases, the results are quite good.

Figure 4 shows the density of the semi-transparent slab as a function of phase and also the densities obtained by Fe line analysis (Schwarzschild, et al, 1948). Note the relatively good agreement and also the amount of detail. The shock and rarefaction labels correspond to those on the model results in Figure 2. One would expect to see a transient density increase after each shock wave emerges. Figure 4 appears to confirm this expectation.

The dynamic atmosphere technique also yields the relative radius as a function of phase. An absolute normalization of the radius can be obtained by two methods (Hillendahl 1968). The results of this analysis are

Table 1: Example of a Dynamic Atmosphere (Phase 0.10)

| Wavelength Å | $B(T_b)$ | Abs. Coeff. | $B(T_a)$ | Calc. F | Obs. F | Calc. F/Obs. F | |
|---|---|---|---|---|---|---|---|
| 10309 | 40.74 | 7.168(-12) | 14.92 | 21.479 | 21.479 | 1.000 | |
| 7194 | 52.13 | 8.148(-12) | 13.85 | 22.056 | 22.285 | 0.999 | |
| 5714 | 53.64 | 7.088(-12) | 10.60 | 21.680 | 21.678 | 1.000 | |
| 5128 | 51.89 | 6.638(-12) | 8.65 | 20.693 | 20.702 | 1.000 | |
| 5000 | 51.24 | 6.544(-12) | 8.19 | 20.372 | 20.324 | 1.002 | |
| 4901 | 50.66 | 6.474(-12) | 7.82 | 20.095 | 19.953 | 1.007 | |
| 4784 | 49.88 | 6.393(-12) | 7.38 | 19.727 | 19.055 | 1.035 | ** |
| 4673 | 49.04 | 6.319(-12) | 6.94 | 19.334 | 19.589 | 0.987 | |
| 4566 | 48.14 | 6.252(-12) | 6.53 | 18.920 | 19.055 | 0.993 | |
| 4464 | 47.19 | 6.192(-12) | 6.12 | 18.484 | 18.031 | 1.025 | ** |
| 4367 | 46.20 | 6.140(-12) | 5.74 | 18.209 | 17.702 | 1.018 | |
| 4255 | 44.96 | 6.087(-12) | 5.30 | 17.460 | 17.539 | 0.995 | |
| 4166 | 43.90 | 6.051(-12) | 4.95 | 16.969 | 17.219 | 0.985 | |
| 4081 | 42.80 | 6.022(-12) | 4.62 | 16.463 | 16.293 | 1.010 | |
| 4032 | 42.14 | 6.009(-12) | 4.43 | 16.154 | 15.417 | 1.048 | *** |
| 3906 | 40.34 | 5.986(-12) | 3.95 | 15.311 | 13.677 | 1.119 | *** |
| 3846 | 39.44 | 5.981(-12) | 3.73 | 14.881 | 12.942 | 1.150 | *** |
| 3774 | 38.29 | 5.618(-12) | 3.46 | 15.060 | 10.578 | 1.425 | *** |
| 3703 | 37.14 | 5.622(-12) | 3.21 | 14.504 | 6.792 | 2.136 | *** |
| 3636 | 35.99 | 1.437(-11) | 2.98 | 5.549 | 5.495 | 1.010 | |
| 3571 | 34.85 | 1.396(-11) | 2.76 | 5.421 | 5.346 | 1.014 | |
| 3508 | 33.71 | 1.359(-11) | 2.55 | 5.293 | 5.297 | 0.999 | |
| 3448 | 32.58 | 1.325(-11) | 2.36 | 5.163 | 5.754 | 0.897 | ** |

$T_b = 8400^\circ K$ $T_a = 5500^\circ K$ RR = 0.9829

$U_s = 3.56\ (+06)$ $\Delta X = 1.247\ (+11)$ $U_a = 2.00\ (+06)$

** Difference greater than 2 percent, reason unknown

*** Balmer line effect

Units for Planck functions and fluxes are arbitrary scale.

Table 2: Dynamic Model Atmosphere Parameters for Eta Aquilae

| Phase | $T_b$ ($^oK$) | $T_a$ ($^oK$) | $\rho_a$ (gm $cm^{-3}$) | $\Delta X$ (cm) | Relative Radius | Velocity | Quality of Result |
|---|---|---|---|---|---|---|---|
| 0.55 | 11000 | 5300 | 1.20(-9) | 4.41(11) | 1.052 | 25.2 | good |
| 0.60 | 10800 | 5200 | 1.00(-9) | 6.71(11) | 1.051 | 16.9 | good |
| 0.65 | 12800 | 5300 | 8.37(-10) | 8.75(11) | 1.024 | ---- | good |
| 0.70 | 16600 | 5300 | 8.37(-10) | 1.05(12) | 1.020 | ---- | good |
| 0.75 | 11900 | 5300 | 1.44(-9) | 3.78(11) | 0.979 | ---- | good |
| 0.80 | 11000 | 5500 | 2.48(-9) | 1.02(11) | 0.966 | -1.57 | good |
| 0.85 | 9600 | 5900 | 1.72(-9) | 6.36(10) | 0.908 | 7.92 | good |
| 0.90 | 9000 | 5700 | 2.48(-9) | 3.40(10) | 0.932 | 25.8 | poor |
| 0.95 | 8300 | 5800 | 1.43(-9) | 3.20(10) | 0.890 | 36.4 | excellent |
| 0.00 | 8700 | 5400 | 5.78(-10) | 3.67(11) | 0.929 | 43.5 | poor |
| 0.05 | 8050 | 5700 | 8.37(-10) | 5.70(10) | 0.930 | 37.1 | poor |
| 0.10 | 8400 | 5500 | 1.00(-9) | 1.24(11) | 0.983 | 35.7 | good |
| 0.15 | 8400 | 5900 | 2.07(-9) | 2.53(10) | 0.959 | 31.3 | poor |
| 0.20 | 9600 | 5800 | 3.00(-9) | 3.02(10) | 1.009 | 32.6 | poor |
| 0.25 | 11000 | 5900 | 3.00(-9) | 3.24(10) | 1.002 | 36.5 | poor |
| 0.30 | 10600 | 5900 | 2.50(-9) | 4.09(10) | 1.001 | 31.9 | good |
| 0.35 | 10000 | 5800 | 2.07(-9) | 5.92(10) | 1.015 | 26.4 | good |
| 0.40 | 9600 | 5600 | 1.20(-9) | 2.00(11) | 1.049 | 23.5 | good |
| 0.45 | 9400 | 5300 | 1.20(-9) | 3.27(11) | 1.056 | 21.1 | good |
| 0.50 | 10000 | 5400 | 1.44(-9) | 2.45(11) | 1.038 | 23.1 | good |

compared with other results (Whitney 1955) for Eta Aquilae in Figure 5.

The method of dynamic atmospheres should not be interpreted as a theoretical modeling technique, but rather as a means of interpreting observations of the stellar continuum. The agreement obtained for Eta Aquilae apparently occurs since hydrodynamic motion is responsible for the creation of the atmospheric profiles. Numerous attempts to fit the observed continuum from cepheids with radiative equilibrium model atmospheres have not proven successful over the entire width of the observed spectrum.

The cepheid models computed with the SUPER NOVA code also predict some interesting results relative to the line spectra from cepheids. During the first half of the period, when rarefaction waves dominate the atmosphere (Fig. 2), the atmospheres exhibit a large velocity gradient in which the particle velocity within the unloading region increases almost linearly with radius. Such a velocity gradient should have an observable effect on the shapes of spectral lines formed in this region of the star.

Line profiles have been computed (Hillendahl 1969) from the atmospheric profiles produced by the SUPER NOVA code. Figure 6 shows the computed profile for the $\lambda$ 4508 Å line of Fe II and is labeled V=F(R). Other profiles shown were obtained by numerical experimentation in which the velocity was set to various constant values throughout the atmosphere.

In the computed profile, the velocity distribution is seen to produce an asymmetry in the line and to approximately double the equivalent width. A satellite line is obtained at approximately twice the Doppler shift of the main line. This results from velocity doubling in the unloading wave (Hillendahl 1970) and is similar to features often seen in stars above the main sequence - whether or not they are "pulsating".

Figure 7 shows computed lines for the $H_\beta$ and Ca II K lines. The noticeable feature of the $H_\beta$ line is the depression of the continuum over a broad region of the spectrum. Balmer line blanketing is thus predicted by the models and is apparently confirmed by the results of Table 1. The Ca II K line is quite broad and shows a weak red shifted emission core. This emission core results from the slight temperature inversion in the outermost region of the model (Fig. 3). The dashed line shows the change in the K line profile when this outer shell in the model is arbitrarily removed during the line profile calculation. The blue shifted profile with a red shifted core seems to be in agreement with the observations of Jacobsen (1956).

The SUPER NOVA model calculations also achieve some success in predicting the complex behavior which occurs when the cepheid atmosphere collapses. Figure 8 shows the predicted structure of the atmosphere for a 7.6 day cepheid at several phases. The heavy lines indicate various shock fronts and the photosphere. The finer lines are radius-vs-time trajectories for various mass

zones in the model. The numerical values indicate the local particle velocities in various regions.

Figure 9 shows the observed $H_\alpha$ profile for SV Vul as observed by Grenfell and Wallerstein (1969). The doppler shift measured from FeI lines is indicated by the arrow. (Note that the observed radial velocities would be approximately 17/24 of the particle velocities predicted by the model. However, the velocity applitude of SV Vμl is approximately 24/17 that of the 7.6 day model, so that the two effects tend to compensate).

At phase 0.84, the model predicts three distinct layers of material having velocities corresponding very well with the doppler shifts of the observed line cores.

The author's purpose in this presentation has been to demonstrate that relatively complex phenomena occurring in cepheid atmospheres. It is hoped that this discussion might provide guidance to cepheid observers in planning their programs and in limiting the duration of their observations so that they isolate in time the various features predicted by the models.

## REFERENCES


Brode, H. L. 1955, J. Appl. Phys. 26, 766.

Brode, H. L. 1956, RM-1824-AEC.

Brode, H. L. 1957, RM-1825-AEC.

Brode, H. L. 1958, RM-2247.

Brode, H. L. 1959a, RM-2248.

Brode, H. L. 1959b, RM-2249.

Brode, H. L. ed., 1965, "Reliability of Current Nuclear Blast Calculations", Proceeding, of the DASA Conference on Nuclear Weapons Effects and Re-Entry Vehicles, DASA Report 1651 (Classified)

Christy, R. F. 1964, "Rev. Mod. Phys. 36," 555.

Christy, R. F. 1967, "Computational Methods in Stellar Pulsation", in Vol. 7 of "Methods in Computational Physics" ed. B. Alder. Academic Press, New York.

Christy, R. F. 1968, Private Communication.

Grenfell, T. C., and Wallerstein, G. 1969, P.A.S.P. 81, 732.

Henyey, L. G., LeLevier, R., Levee, R. D., Böhm, K. H., and Wilets, L. 1959, Astrophys. J. 129, 628.

Hillendahl, R. W. 1959, "Characteristics of the Thermal Radiation from Nuclear Detonations" AFSWP 902, Vols. I, II, III.

Hillendahl, R. W. 1962, Appendix B of "The Spectral Absorption Coefficient of Heated Air", DASA 1348, Unclassified.

Hillendahl, R. W. 1964, "Approximation Techniques for Radiation - Hydrodynamics Calculations", DASA 1522, Unclassified.

Hillendahl, R. W. 1965a, Proceedings of the Workshop on the Interdisciplinary Aspects of Radiative Transfer, J.I.L.A., ed. R. Goulard.

Hillendahl, R. W. 1965b, "Theoretical Models for Nuclear Fireballs" Part A, Lockheed Palo Alto Research Laboratories, DASA 1589 - LMSC BOO 6750, Unclassified.

Hillendahl, R. W. 1966, "Theoretical Models for Nuclear Fireballs (U)", DASA report 1589, Part B in 40 volumes, (Classified).

Hillendahl, R. W. 1968, "Atmospheric Phenomena in Classical Cepheids", dissertation, University of California at Berkeley.

Hillendahl, R. W. 1969, NBS Special Publication 332, "Spectrum Formation in Stars With Steady-State Extended Atmospheres".

Hillendahl, R. W. 1970, P.A.S.P. 82, 1231.

Jacobsen, T. S. 1956, Pub. Dom. Ap. Obs. Victoria, 10, 145.

Oke, J. B. 1961, Ap.J. 133, 90.

Richtmyer, R. D., and Von Neumann, J. 1950, J. Appl. Phys. 21, 232.

Richtmyer, R. D. and Morton, K. W. 1967, "Difference Methods for Initial Valve Problems", Second Ed., Interscience Publishers, New York.

Simpson. E. 1973, Science Applications, Inc., Palo Alto, California - Private Communication.

Schwarzschild, M., Schwarzschild, B., and Adams, W. S. 1948, Ap.J. 108, 207.

Von Neumann, J., and Richtmyer, R. D. 1950, J. Appl. Phys. 21, 232.

Whitney, C. 1955, Ap.J. 121, 682.

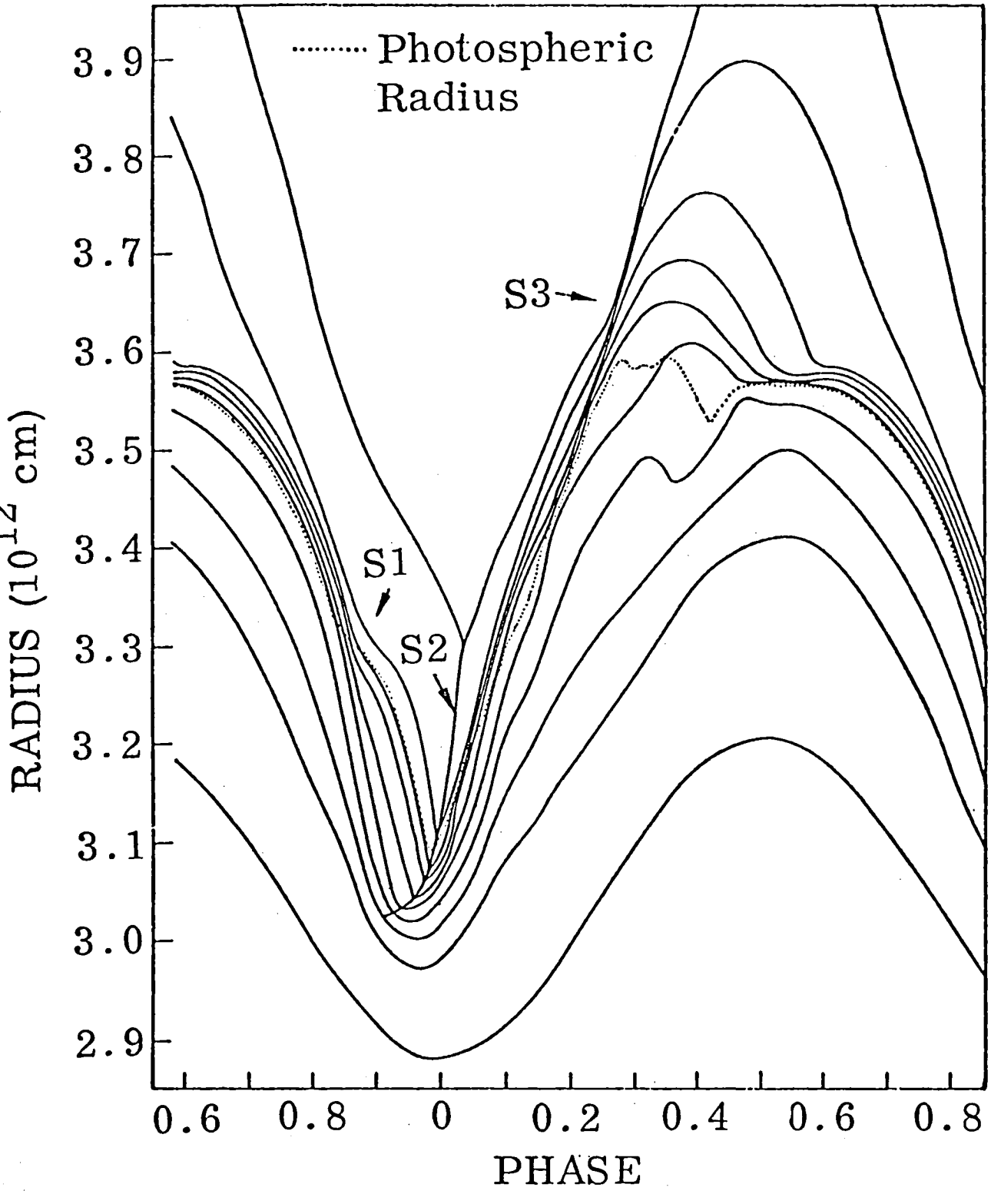


Figure 1. Radius-versus-Phase for a Cepheid Model

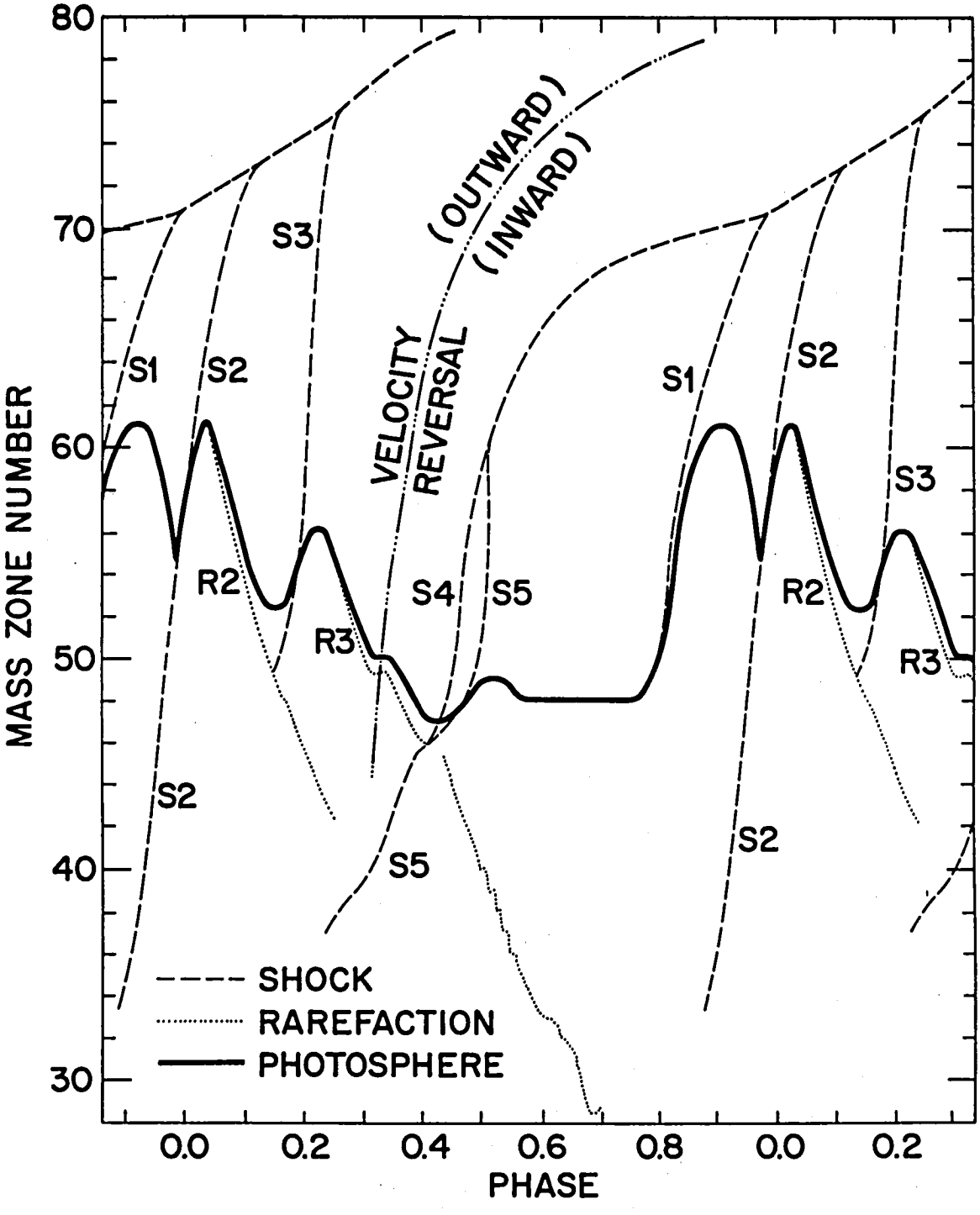


Figure 2. Diagnostic Diagram for a Cepheid Model

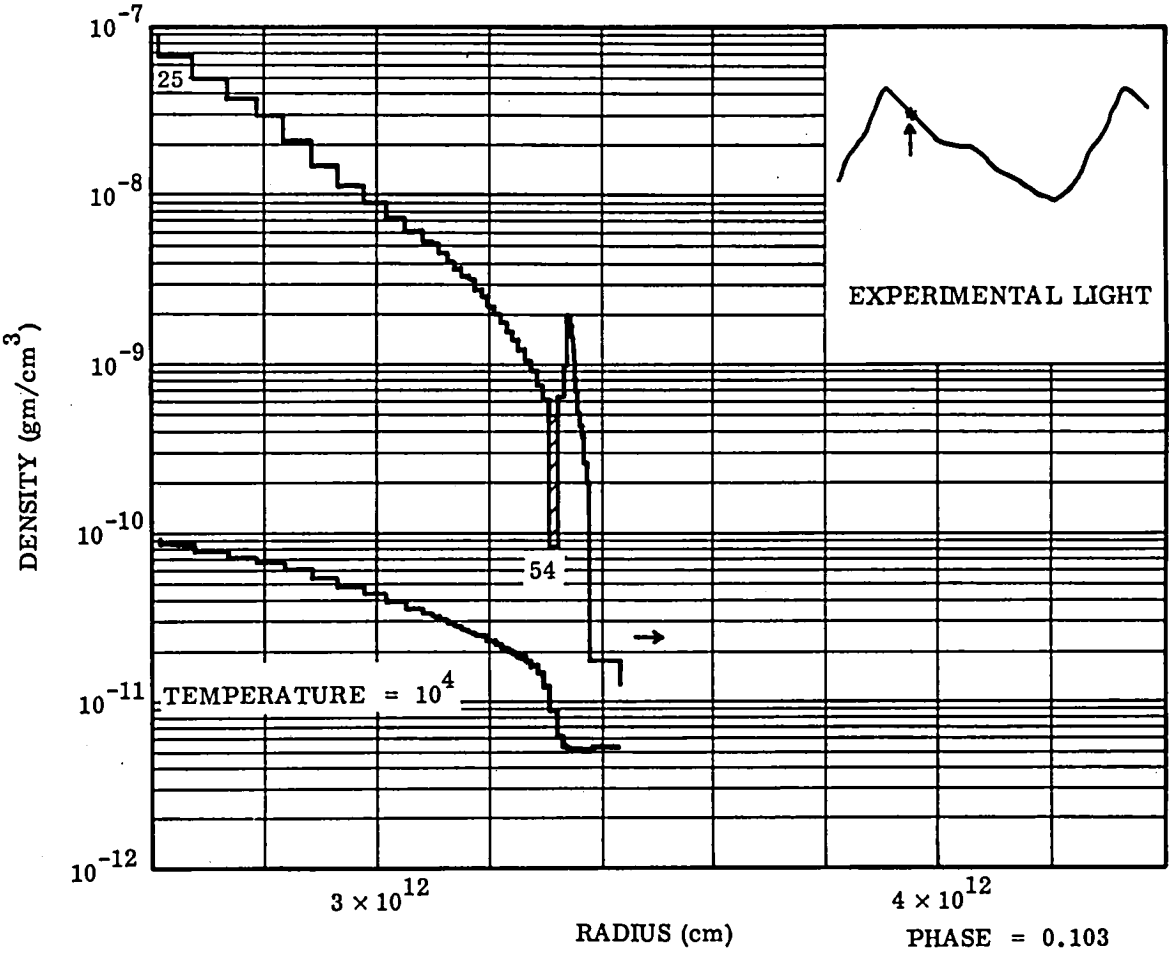


Figure 3. Atmospheric Profiles at Phase 0.103

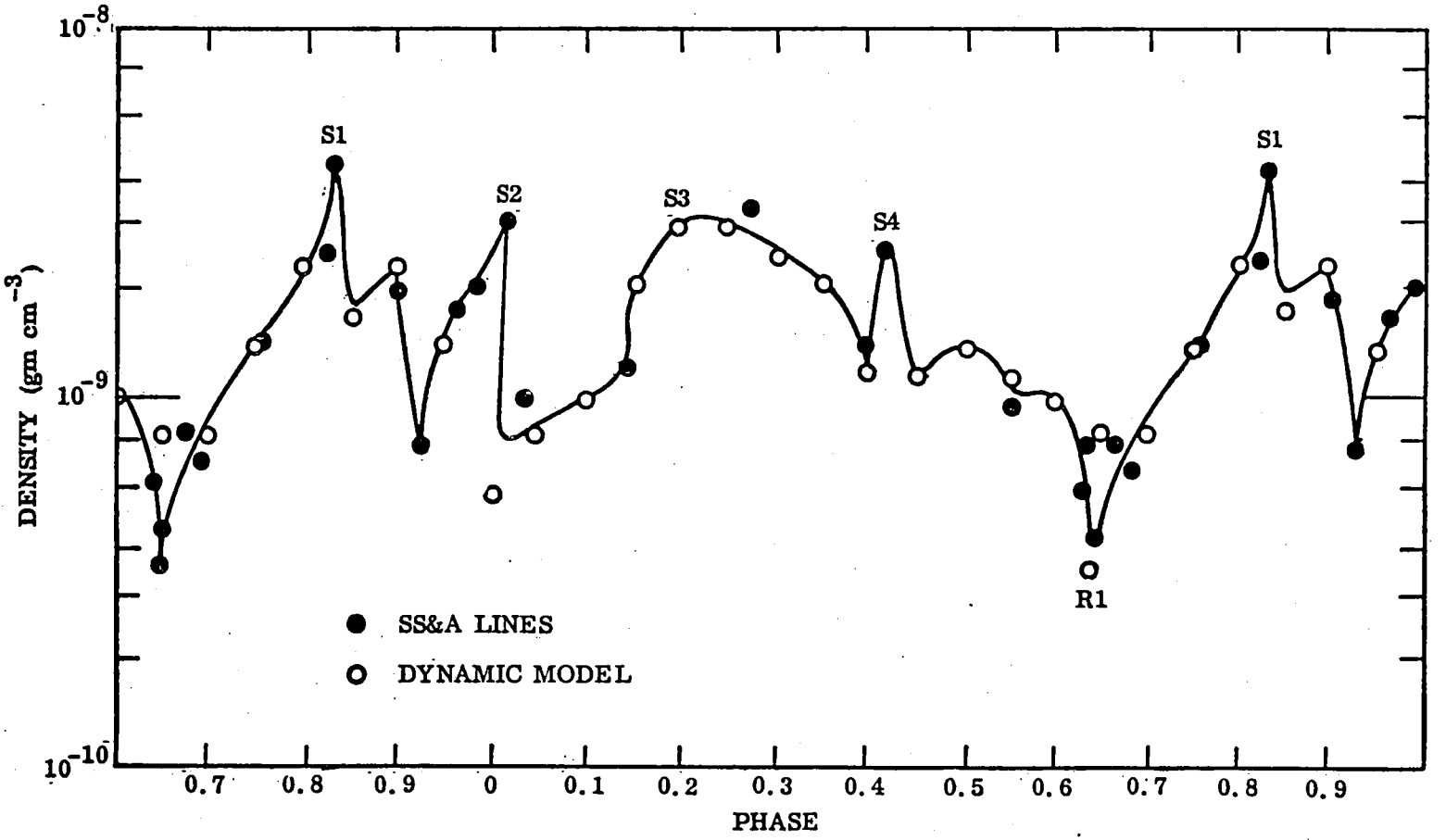


Figure 4. Density-versus-Phase for Eta Aquilae as Deduced from Two Types of Observations

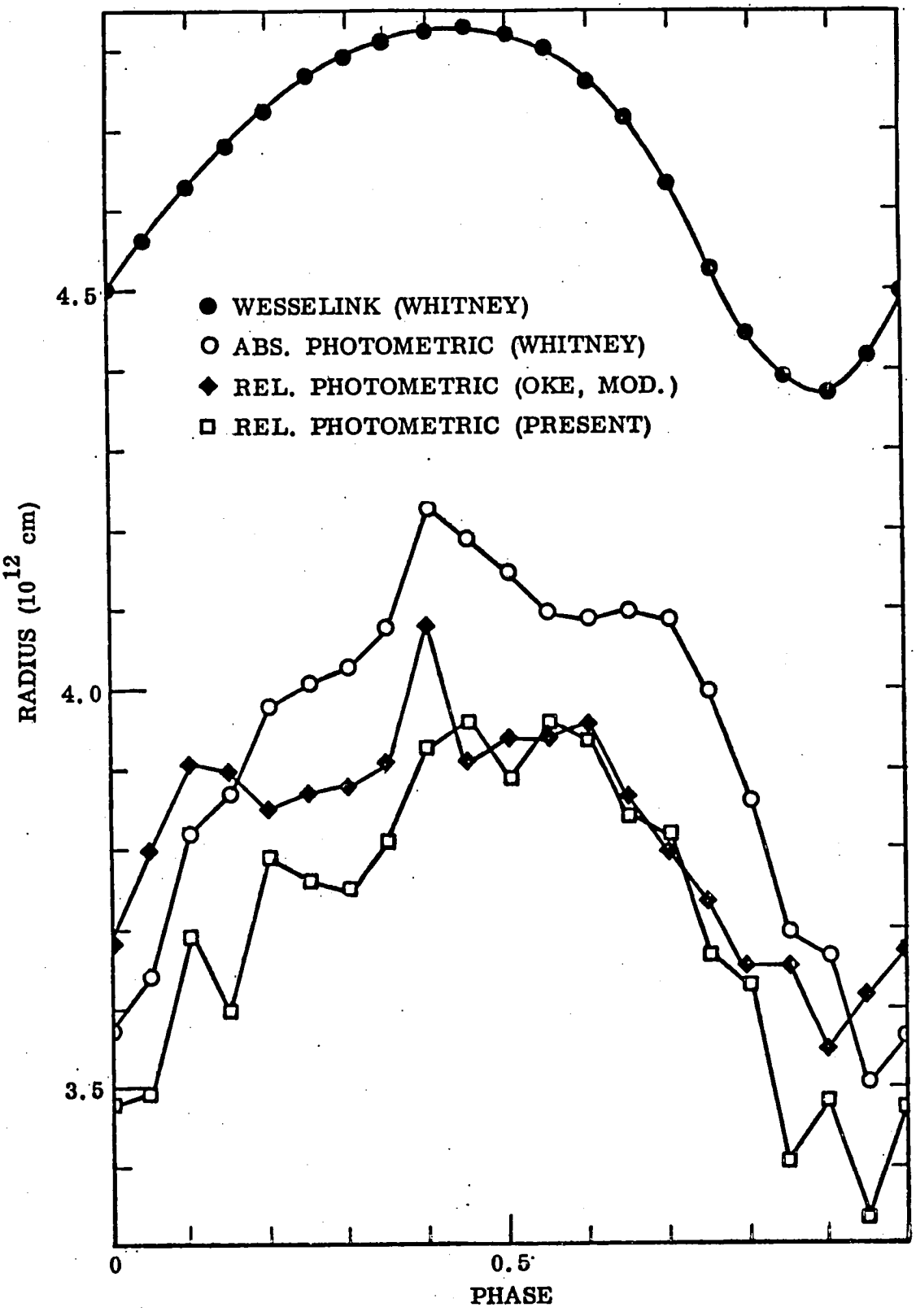


Figure 5. Radius-versus-Phase for Eta Aquilae

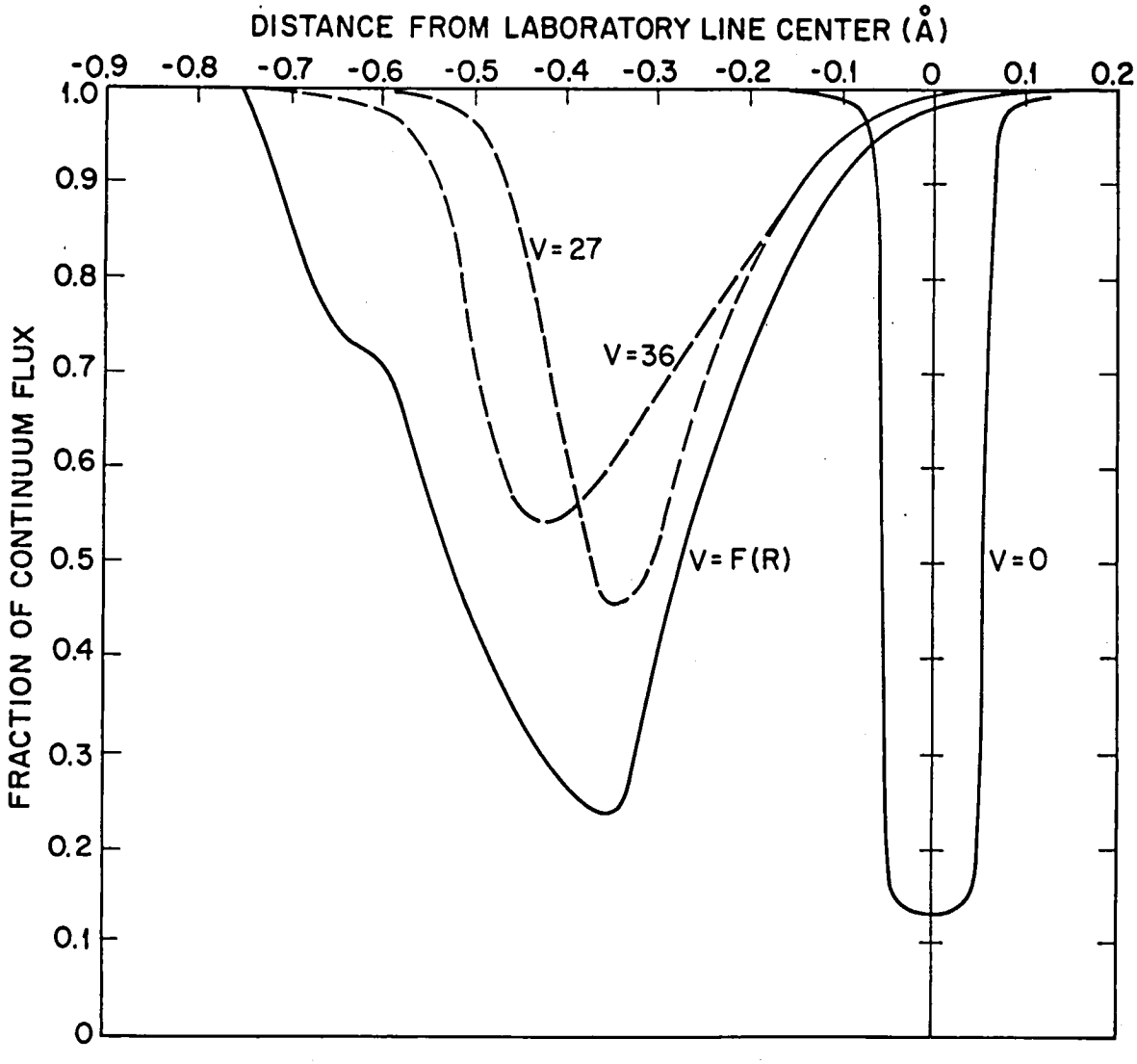


Figure 6. Computed Line Profiles for λ4508Å Fe I

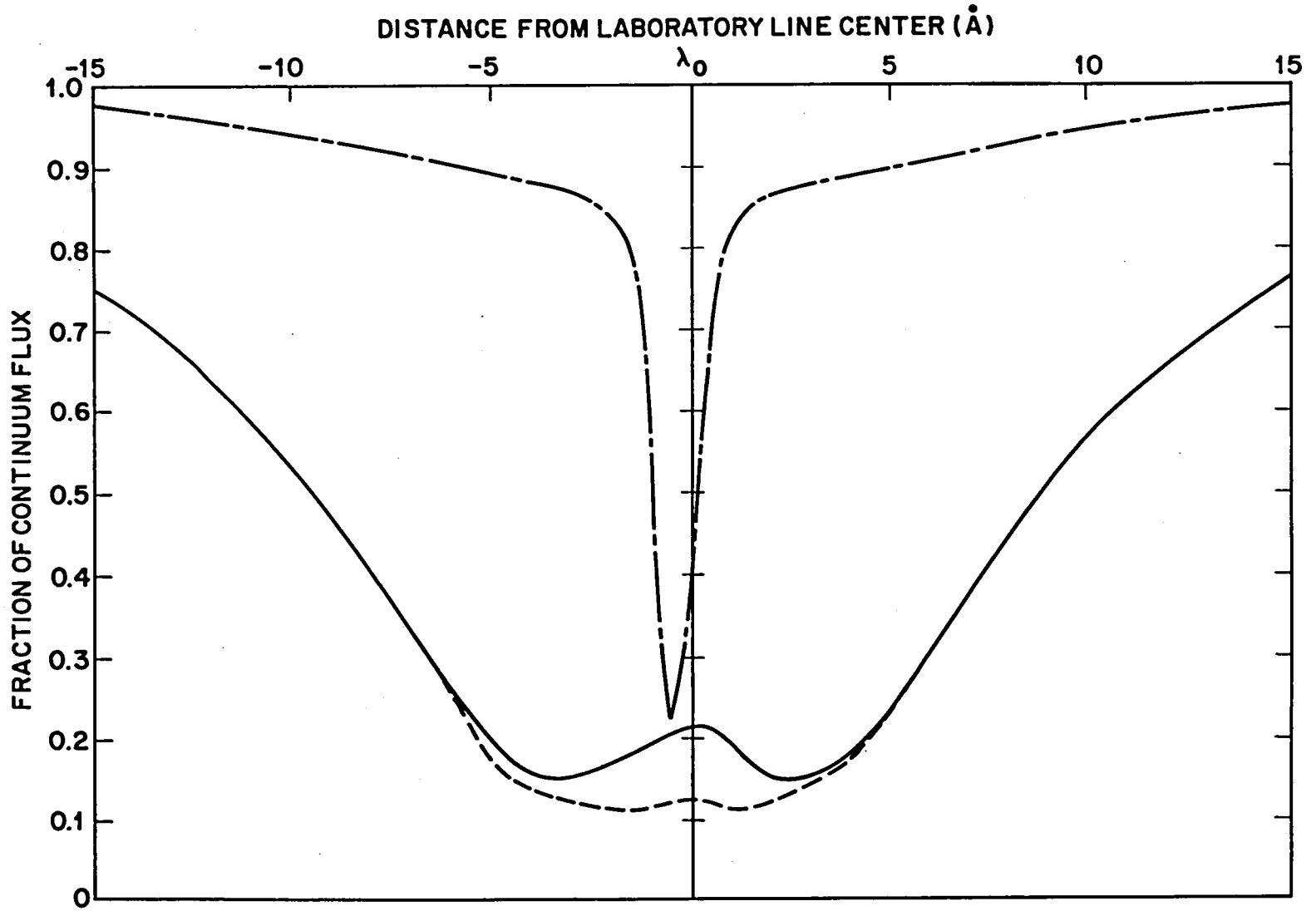


Figure 7. Computed Line Profiles for Hβ and Ca II K

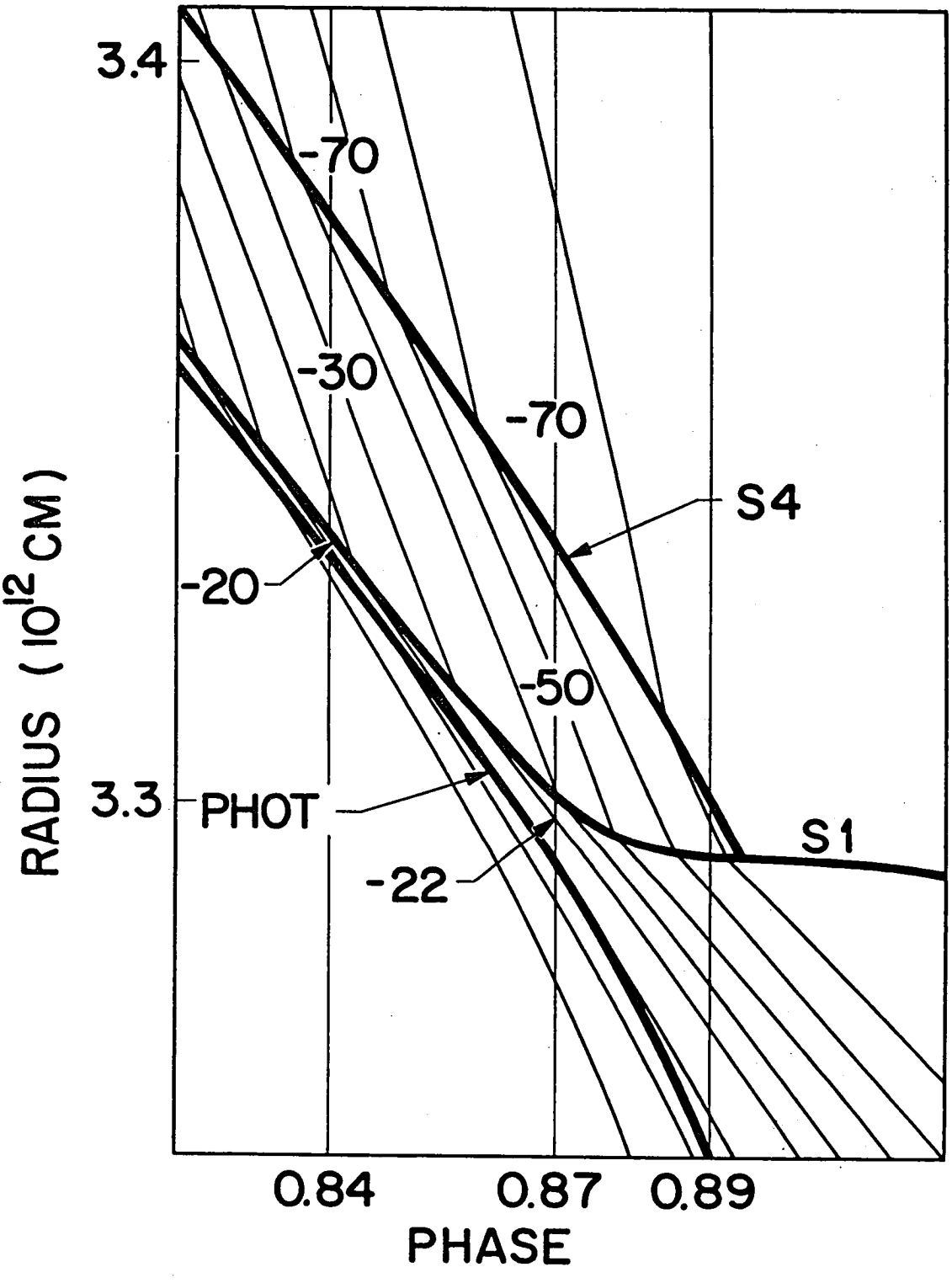


Figure 8. Atmospheric Structure During Collapse

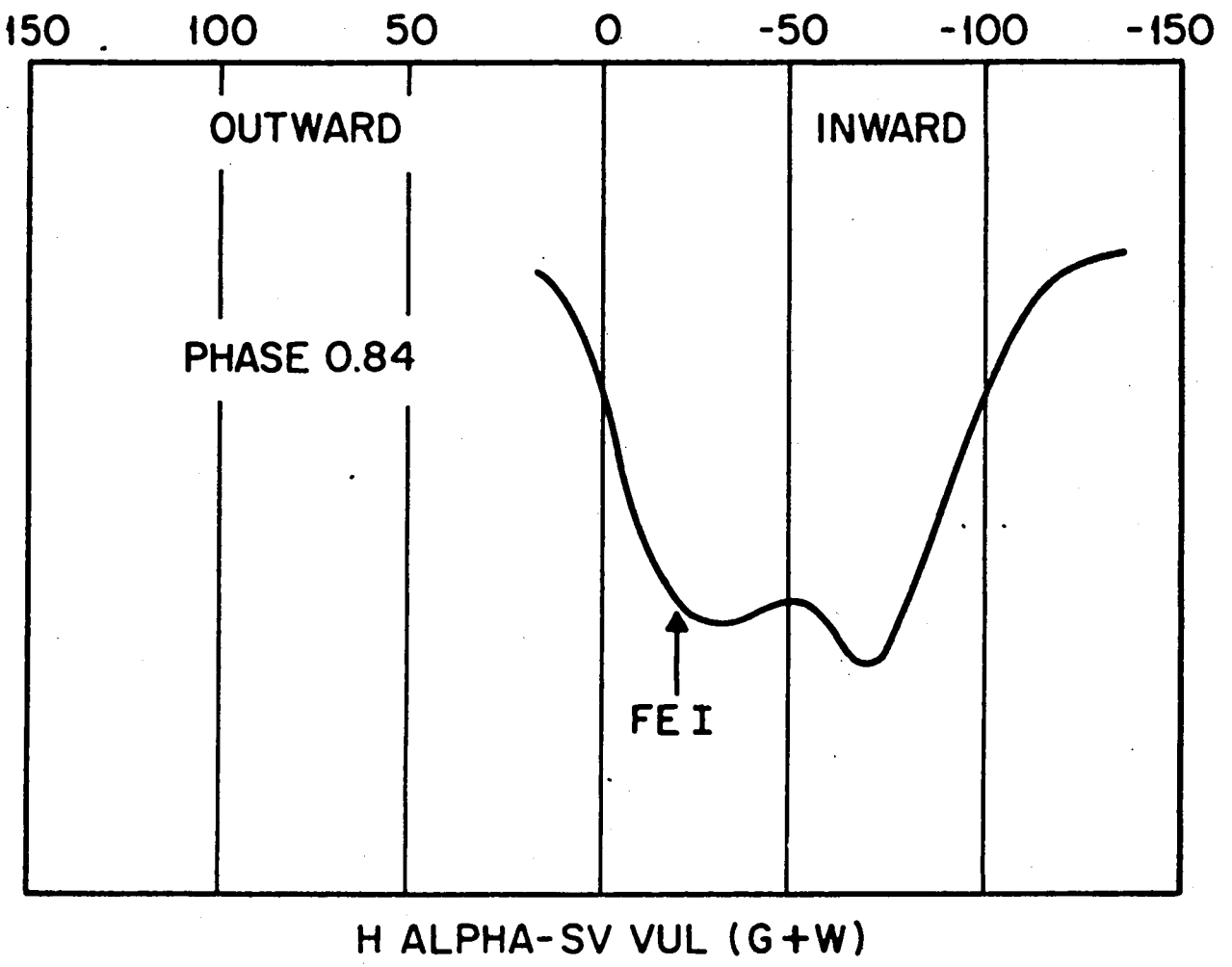


Figure 9. Observed Line Profiles SV Vul

## Discussion

Adams: Do you have anything to say about the mass anomally?

Hillendahl: I'm prejudiced. I used the low Christy mass. I did a paper in 1955 that says the masses are about one half of what they should be. This technique I've talked about -- trying to use the maximum possible observational data with the minimum possible theoretical interpretation -- leads to the same sort of result. What you are doing is taking lines that you hope are in the photosphere and following them for a particular part of the phase, and if you integrate the velocity over that time, you get the absolute displacement of that part of the cycle. If you differentiate the velocity you get g. The problem is then that you have absolute displacement over part of the cycle but you don't have radius, so you have to go to some other technique to get the relative radius. If you do this, you end up with masses that are too small compared to the evolutionary mass.

Pel: At the last Goddard conference in this series, Hutchinson, Hill and Lilly presented some observational data for β Dor from the OAO-2 satellite. They thought they saw sharp blue peaks on the rising branch of this 10-day Cepheid, which they interpreted as evidence for shock waves. Together with J. Lub and J. Van Paradijs, I observed this star with the ANS satellite. I think we have much better data and we do not see these blue peaks. On the other hand, we have problems fitting the whole rising branch of the light curve with the Kurucz models. I don't find a satisfactory equilibrium model that fits the energy distribution from 5500Å to 1800Å. So there is some evidence for non-equilibrium radiation.

Hillendahl: Well, it's a question of whether it's non-equilibrium radiation in the Dick Thomas sense or LTE radiation from a moving gas.

Pel: We can't distinguish between those two things. What we can say is that there don't seem to be pronounced short-lived peaks on the light curve there, but the energy distribution cannot be represented well by a hydrostatic equilibrium model atmosphere.

Hillendahl: No. In all deference to Stromgren, I think he was wrong. I think Karl Schwarzschild was right. In 1905, his two-stream method was for convective atmospheres, not for radiative ones. At the time I did this work, the OAO-2 information on Cepheids was just beginning to come down. I think they did see a little blip at 0.95, which is about where I would expect to see the shock. One of the things you must be careful of in a model calculation is the zoning. Simply because your code says there is a shock wave, it doesn't necessarily mean you can see it. In a fireball model where your zoning is a 1 meter scale, these effects are on a scale of 0.1 mm. There is a radiative structure in which the gas dynamic discontinuity is embedded. There is a paper by J. Zinn and R. C. Anderson (Phys. Fl. 16, Nov. 10, 1973), in which they have done the modeling of a radiative shock front. Shock fronts don't always have that great brightness you might expect them to have. Only under certain relationships between the density of the gas and the radiative mean free path will you see the shock front itself. The rest of the time it's going to be embedded in radiative precursors. So my guess is that your ability to see shock waves is going to be very limited. Just a little bump on the curve. Most of the gross features that you see that last for days and

days are caused by the progression of the photosphere inward due to hydrodynamic expansion of the gases behind the front, and sometimes rarefaction waves. I think you can show this quite easily.

J. Wood: In your fireball graph you mentioned a Christy reflection. What's it reflecting off of?

Hillendahl: A fireball is quite different from a star. A star has a very dense center. A fireball is essentially evacuated in the center, but nonetheless, the shock wave does reflect off the center. It makes a difference (sort of a coefficient of restitution) what sort of materials and structure you use. Particularly in the outer layers, it has been shown by comparison with experiment that the equation of state is absolutely sacred.